Thermal Analysis of Salient Pole Synchronous Machines by Multiple Model Planes Approach

P. Shams Ghahfarokhi, A. Kallaste, A. Podgornov, A. Belahcen, T. Vaimann, O. Kudrjavtsev

Abstract -- **This paper presents the lumped parameter thermal network of high power salient pole synchronous machine. For this purpose, the multi-model planes approach is implemented. Accordingly, the active machine parts divided into three planes, and to model the end windings, two other planes are added to model the driven and non-driven end-windings regions of the machine. In addition, it describes the challenges and provides solutions to dominate them during thermal modeling of the electrical machine by the multi-model planes approach. Finally, the proposed method is validated experimentally on open self-ventilated salient pole synchronous machine, and good correspondence between the analytical and experimental results is obtained.**

Index Terms**—AC machines, cooling, electrical machines, equivalent circuit, temperature measurement, thermal analysis**

I. INTRODUCTION

The high megawatt salient pole synchronous machines are the conventional high power machinery for the industrial application. These machines with a salient pole rotor provide high efficiency, low noise, and vibration; however, they should have excellent thermal stability.

To consider the thermal stability of the machine under the design process, the thermal analysis of the machine in parallel with the electromagnetic design is necessary. Analytical and numerical thermal methods are two conventional thermal analysis approaches[1]-[4]. According to the advantages of analytical lumped parameter thermal networks such as fast computation with reasonable accuracy, this method attracts attention to model the heat transfer and thermal analysis of electrical machines in both research and industrial sections [5].

An open self-ventilated (OSV) system is the standard cooling method, which is implemented on these types of machines. Due to the cost-effective and straightforward design of the OSV cooling system, this cooling system is the noteworthy cooling method [6]. In this cooling system, the fluid flow (air) produced by a radial shaft-mounted fan is passed through the inner parts of the machine by three parallel paths; stator cooling ducts, rotor cooling ducts, and air gap [4].

Several different industrial and research studies considered heat transfer and the thermal model of the OSV cooling method [7]-[10]. Most of them developed their lumped parameter thermal networks ([10]-[13]) based on the generic cylinder element method presented by Mellor et al. in [14]. Furthermore, some research papers provide ([15],[16]) multiple planes approach, but this method has not been implemented for the high power machines in the range of megawatt.

In this paper, the analytical lumped parameter thermal network of the OSV machine by the multiple model planes approach is presented. The objective of this study is to enhance knowledge in thermal design and analysis of the electrical machine and develop the analytical thermal analysis tools for the OSV electrical machines with a particular focus on non-salient pole synchronous machines. The research focuses on existing challenges and problems in ongoing method development. The main objective is to develop a scientifically sound method that can be used in the thermal design and analysis of the OSV electrical machines.

For the research purposes, the multiple model planes approach described in this study is applied to a four poles two MW, 10.5 kV, 50 Hz, salient pole synchronous machines with 'F' insulation class. The analytical method for calculation of the heat transfer coefficient is developed, and the estimation of its parameters is thoroughly described. To validate the method, a test bench is set up, and measurements are conducted. The experimental results are then compared to these from the proposed method.

II. THERMAL MODEL DESCRIPTION

The multiple model planes approach is a three-dimensional method to model the heat transfer and thermal analysis of the electrical machine. In this method, the heat transfer in the machine is modeled in the axial and radial direction. This method enhances the accuracy and resolution of the temperature distribution model of the machine by providing the sizeable thermal network involved in the high number of nodes and thermal paths. Accordingly, the active machine section is divided into three principal planes (Planes 'A', 'B,' and 'C'). Besides, to model the heat transfer of the end windings, two other plans ('D' and 'E') are added to the model

This work has been supported by the European Regional Development Fund within the Activity 1.1.1.2 "Post-doctoral Research Aid" of the Specific Aid Objective 1.1.1 "To increase the research and innovative capacity of scientific institutions of Latvia and the ability to attract external financing, investing in human resources and infrastructure" of the Operational Programme "Growth and Employment" (No.1.1.1.2/VIAA/3/19/501).

P. Shams Ghahfarokhi is with Riga Technical University and Tallinn University of Technology, Riga, Latvia (e-mail: payam.shams@taltech.ee).

A. Kallaste is with Tallinn University of Technology, Tallinn, Estonia. (e-mail: ants.kallaste@taltech.ee).

A. Podgornov is with Riga Technical University, Riga, Latvia (e-mail: andrejs.podgornovs@rtu.lv).

A. Belahcen is with Aalto University and Tallinn University of Technology, Espoo, Finland (e-mail: anouar.belahcen@aalto.fi).

Toomas Vaimann is with Tallinn University of Technology, Tallinn, Estonia. (e-mail: toomas.vaimann@taltech.ee).

O. Kudrjavtsev is with ABB AS Electrical Machines Factory, Tallinn, Estonia. (e-mail: Oleg.Kudrjavtsev@ee.abb.com).

978-1-7281-9944-3/20/$31.00 ©2020 IEEE

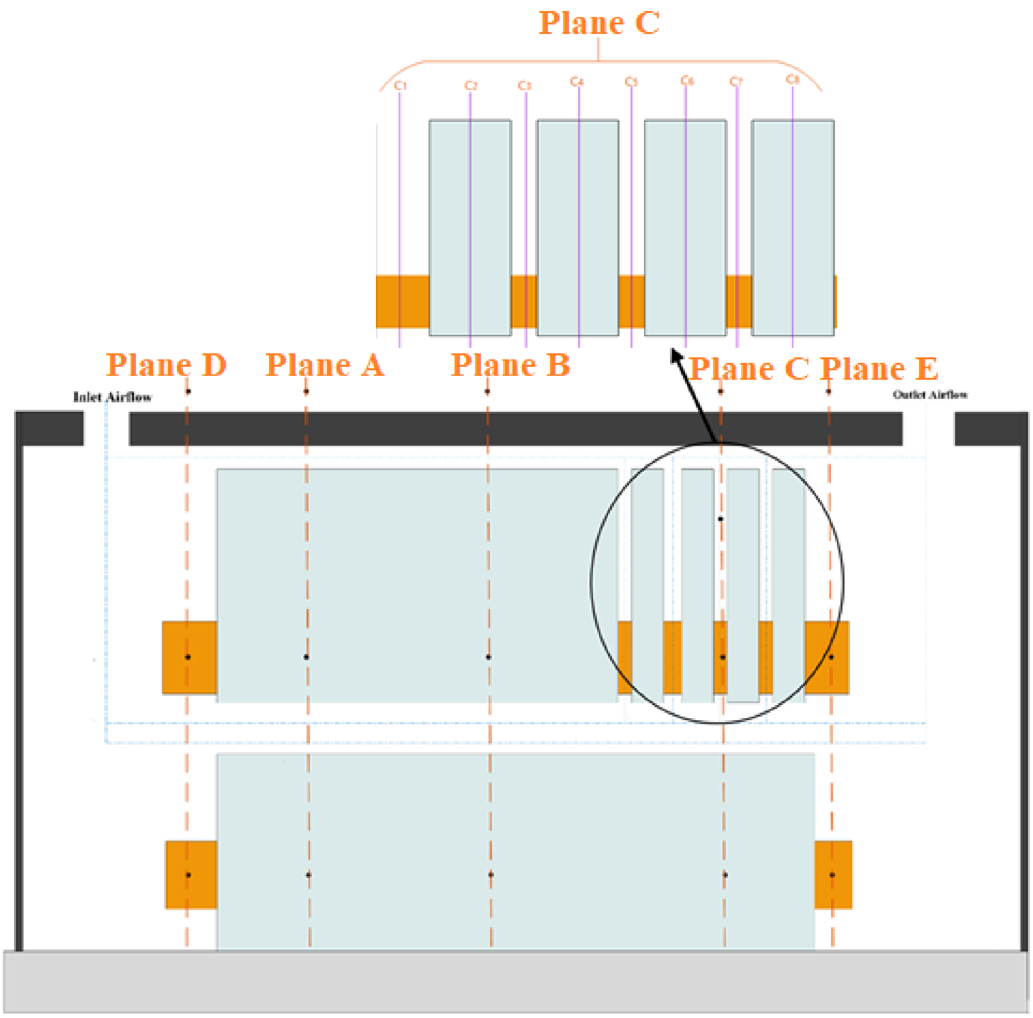

Fig. 1. Multiple model plane thermal approach.

-the end winding respectively for driven and non-driven end parts.

In this type of machine, several radial cooling ducts are located in the stator end part to improve the cooling of this section. Consequently, to enhance the resolution of the LPTN, the last plane (plane 'C') of the stator active region is divided into several sub-planes in according to the number of stator radial cooling ducts (Fig . 1).

Each plane consists of the radial LPTN of the machine that is connected to adjusted planes by the interplane thermal resistances. Furthermore, these interplane resistances represented the axial heat transfer paths.

To develop the LPTN of the machine under study by multiple model planes thermal method, the following hypotheses have been assumed.

- In the OSV cooling system implemented on this type of machine, the airflow inside the air gap provides the main cooling path for the stator and rotor; consequently, the amount of heat exchange between the rotor and stator is minimized. Accordingly, it can be assumed that there is no heat exchange between the rotor and stator, and the heat is transferred by airflow inside the air gap. As a result, the rotor and stator are modeled separately.
- The inner heat sources are distributed uniformly.
- According to the periodical symmetries of stator and rotor, we modeled the one stator slot and one-quarter of the rotor.

A. Radial thermal model

Figure 2 presents the steady-state radial LPTN of the active parts of the stator and rotor developed for the machine under investigation. Accordingly, the radial thermal model of the stator consists of five nodal points. In addition, among the different nodes, there are eight thermal resistances to model the heat transfer by the conduction, convection, and radiation. In addition, the rotor thermal model consists of seven nodes, and among the nodes, there are 19 thermal resistances to model the heat transfer in a radial direction for the rotor.

B. Axial thermal mode

Figure 3 presented the axial LPTN of the stator and rotor. To increase the resolution and clarity of the axial LPTN, for the stator, only axial thermal paths of nodes 0, 1, 4, 5, and 6 are illustrated in this figure. Moreover, for the rotor, nodes 0, 1, 5, and 7 are presented. The blue resistances in the axial thermal models present the airflow paths along the axial direction of the stator and rotor to model the temperature rise of the coolant and increasing the accuracy of the model as well as a prediction of the temperature of the outlet coolant.

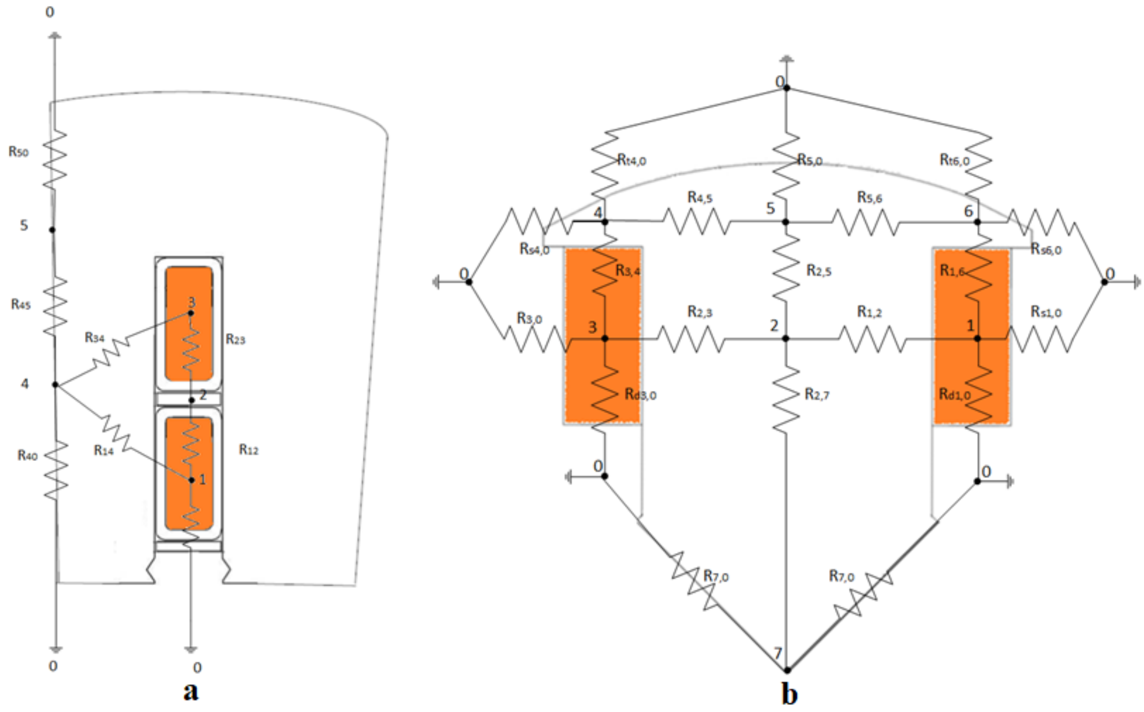

Fig. 2. The steady-state radial thermal models a) stator b) rotor

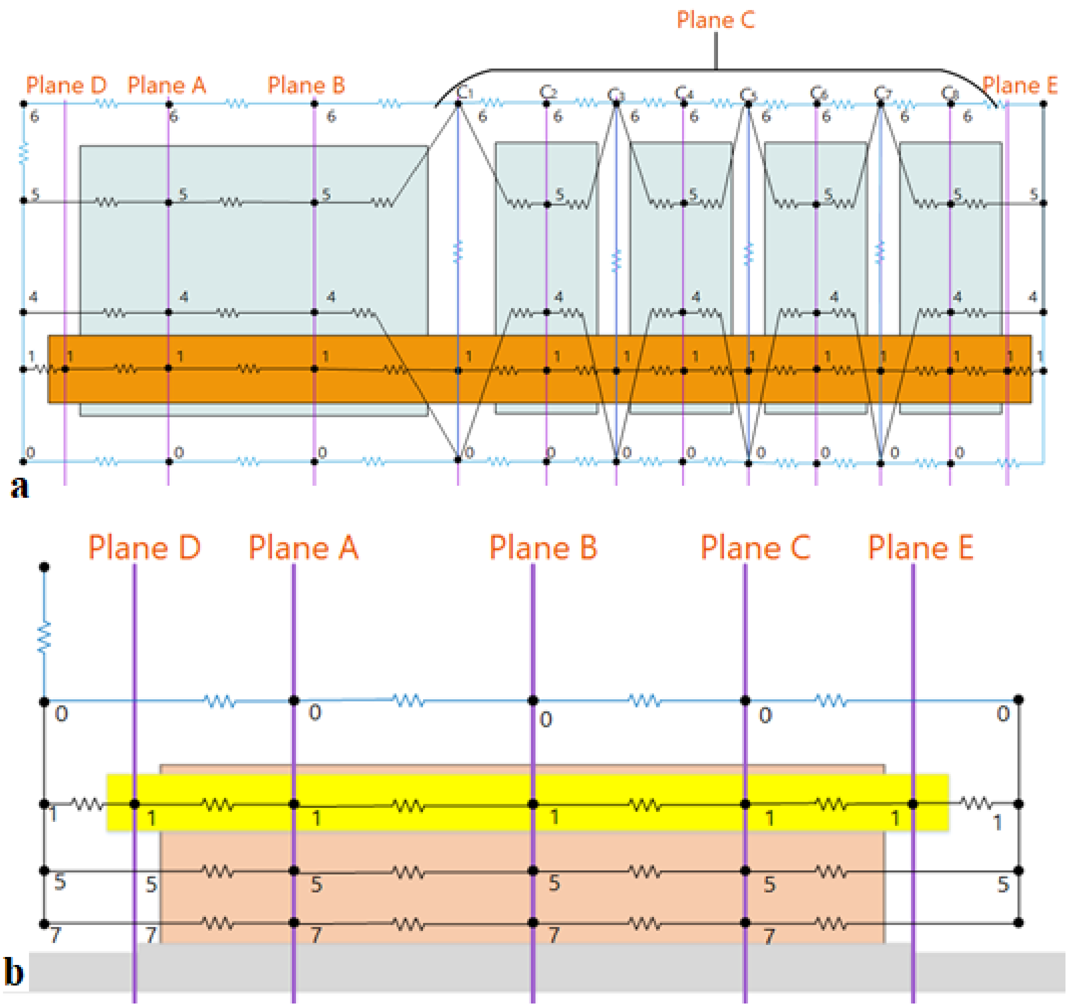

Fig. 3. The steady-state axial thermal model of a) stator b) rotor

III. CRITICAL PARAMETER IN THE THERMAL MODEL

The thermal resistances in the LPTN represent the heat transfer mechanism in the machine [17]. The heat transfer mechanism is divided into three main categories; conduction convection and radiation [4]. The accuracy of the LPTN is highly dependent upon the accurate determination of the parameters. There are several critical parameters in an analytical thermal model of the OSV machines, which play an essential role in the accuracy of the thermal model. In some cases, determining these thermal parameters cannot be calculated by the purely mathematical and analytical approaches. This section describes the critical parameters during the thermal modeling of the machine and provides the solutions to dominate them during the thermal modeling of OSV electrical machines.

Mainly the critical parameters for an analytical thermal model of OSV machines are classified into two categories; critical parameters in the conduction heat transfer and critical parameters of convection heat transfer [4]. Hereafter these parameters are described in detail.

A. A critical parameter of conduction heat transfer

In the conduction heat transfer, the heat is exchanged in the solid material from the hot portion to the cold one by the molecular vibration. The typical form of conduction resistance is defined as:

$$R_{cond} = \frac{L}{kA}, \tag{1}$$

where L is the length of the conduction path, k is the thermal conductivity of a material, and A is the path area.

The challenging parameter in conduction heat transfer is how to model the conduction inside the slots; these sections consist of several materials with the lowest thermal conductivity and high thermal sensitivity. In addition, it has a direct proportion of machine life. The critical parameter in conduction modeling of the slot is to determine the thermal conductivity of the slot. The slot consists of different materials with different thermal conductivity, which makes the slot structure as a non-homogeneous structure [4]. One the method to overcome this complex structure is equivalent thermal conductivity approach, which is proposed by Hashin and Milton as [18]-[20]:

$$k_e = k_{ins} \frac{(1+f_1)k_{\mathrm{cu}}+(1-f_1)k_{\mathrm{ins}}}{(1-f_1)k_{\mathrm{cu}}+(1+f_1)k_{\mathrm{ins}}}, \tag{2}$$

where k_e is equivalent thermal conductivity of slot, k_{cu} is the thermal conductivity of copper, k_{ins} is the thermal conductivity of insulation materials, f_1 is the volume fraction of the conductor in the slot, and f_2 is the volume fraction of the impregnation in the slot (with $f_1+f_2=1$). The other insulation materials are assumed equivalent to the impregnation material, which is a well-justified assumption, as explained in [19].

B. Convection Heat Transfer

In the convection phenomenon, the heat is transferred by the fluid flow motion [21]. The major parts of the heat in the machine are removed by this phenomenon. The convection resistances (R_{conv}) is calculated as:

$$R_{conv} = \frac{1}{h_c A}, \tag{3}$$

where h_c is the convection coefficient, and A is the surface area.

The critical parameter in the calculation of convection resistance is an accurate calculation convection coefficient. This parameter is often calculated by empirical correlations that are developed by dimensionless numbers, e.g., Prandtl (Pr) and Reynolds (Re) numbers [22].

The relationship between the convection coefficient h_c and the Nusselt number (Nu) is defined as [23], [24]:

$$h_c = \frac{\mathrm{Nu}.k}{L}, \tag{4}$$

where k is the fluid flow conductivity, and L is the characteristic length of the surface.

In following the empirical correlations to calculate the convection coefficient from the stationary cooling duct, air gap, end winding, and modeling of the coolant flow temperature rise are described.

1. Stationery cooling ducts

The stationary cooling ducts are located in the stator in either radial or axial orientations. Gnielinski correlation is used to first calculate the Nusselt number and then estimate the convection coefficient. Accordingly, the Nusselt number is defined as [25] :

$$\mathrm{Nu_D} = \frac{\left(\frac{f_{smooth}}{8}\right)(\mathrm{Re}-1000)\mathrm{Pr}}{1+12.7\left(\frac{f_{smooth}}{8}\right)^{0.5}(\mathrm{Pr}^{0.67}-1)}, \tag{5}$$

where f_{smooth} is a friction factor for smooth wall and is calculated as:

$$f_{smooth} = \frac{1}{(1.82\log_{10} Re-1.64)^2}, \tag{6}$$

According to the manufacturing process, the machine's surfaces are not smooth and the roughness of surfaces should be implemented in the calculation of convection coefficient. Accordingly, the Nusselt number of roughness ($\mathrm{Nu_{rough}}$) is defined as [26]:

$$\frac{\mathrm{Nu}_{rough}}{\mathrm{Nu}_{smooth}} = \left(\frac{f}{f_{smooth}}\right)^{0.68\,\mathrm{Pr}^{0.215}}, \tag{7}$$

2. Air gap

Inside the air gap of the OSV machine, we are facing two different fluid flows, the axial flow driven by the fan and the rotational flow due to the rotor rotation. According to Gazley investigation, the convection heat transfer calculated as follow [27]:

$$\mathrm{Nu} = 0.03\left(\frac{D_h V_e}{\vartheta}\right)^{0.8}, \tag{8}$$

$$V_e = \sqrt{U^2 + \left(\frac{V_T}{2}\right)^2}, \tag{9}$$

where D_h is the hydraulic diameter, U is average axial velocity and V_T is the peripheral velocity of the rotor.

3. End-winding

The end winding is one of the critical parts of heat transfer modeling of the electrical machine. In the OSV machine, the radial air flow generated by the end parts of the rotor and the axial flow produced by the fan cool the end winding regions. Furthermore, in this type of machine, the form-wound configuration is applied. In this winding configuration in contrast with random strand winding, the gap among the conductors of the end-winding is not filled by the impregnation materials, and airflow is in direct contact with conductors. As a result, the convection coefficient from the end part of this winding configuration cannot be calculated by the conventional empirical correlation presented in [28], [29]. To calculate the convection coefficient from the end winding of form-wound configuration, the Churchill and Bernstein correlation for the cylinder in crossflow presented in [30] is used. Accordingly, the Nusselt number is defined as:

$$\mathrm{Nu} = 0.3 + \frac{0.62\mathrm{Re}^{0.5}\mathrm{Pr}^{0.33}}{[1+\left(\frac{0.4}{\mathrm{Pr}}\right)^{0.67}]^{0.25}}[1 + \left(\frac{\mathrm{Re}}{282000}\right)^{0.625}]^{0.8}. \quad (10)$$

4. Modeling the coolant flow

In contrast to a totally enclosed fan cooled machine, in the OSV machines, the temperature rise of the coolant flow is high; accordingly, estimating the coolant temperature in different parts of the machine plays an important role in the accuracy of the thermal model [11].

Accordingly, the coolant flow path is added to the LPTN by the blue color. The coolant flow resistance is calculated as following [11]:

$$R_q = \frac{1}{\rho q c_p}, \quad (11)$$

where ρ is mass density, c_p is the specific heat of coolant, and q is the volume of the flow rate of coolant.

IV. Computation of the Nodal Temperature

For the steady-state thermal analysis, the final nodal temperatures of the LPTN can be calculated by the matrix inversion theory. Accordingly, the nodal temperatures of the proposed thermal model are calculated as [11]:

$$[\mathrm{T}] = ([\mathrm{G}] + [\mathrm{G_{fluid}}])^{-1}[\mathrm{P}], \quad (12)$$

where [T] is the temperature column vector, [G] is the thermal conductance matrix, [$\mathrm{G_{fluid}}$] is the cooling matrix, and [P] is the power column vector, which contains the losses at each node. The squared thermal conductance matrix [G] and the squared cooling matrix [$\mathrm{G_{fluid}}$] are defined respectively as [11], [31]:

$$\mathrm{G} = \begin{bmatrix} \sum_{i=1}^{n}\frac{1}{R_{1,i}} & -\frac{1}{R_{1,2}} & \cdots & -\frac{1}{R_{1,n}} \\ -\frac{1}{R_{2,1}} & \sum_{i=1}^{n}\frac{1}{R_{2,i}} & \cdots & -\frac{1}{R_{2,n}} \\ \vdots & \vdots & \ddots & \vdots \\ -\frac{1}{R_{n,1}} & -\frac{1}{R_{n,1}} & \cdots & \sum_{i=1}^{n}\frac{1}{R_{n,i}} \end{bmatrix}, \quad (13)$$

$$\mathrm{G_{fluid}} = \begin{bmatrix} \sum_{i=1}^{n}\frac{1}{R_{q1,i}} & 0 & \cdots & 0 \\ -\frac{1}{R_{q2,1}} & \sum_{i=1}^{n}\frac{1}{R_{q2,i}} & \cdots & -\frac{1}{R_{q2,n}} \\ \vdots & \vdots & \ddots & \vdots \\ -\frac{1}{R_{qn,1}} & -\frac{1}{R_{qn,1}} & \cdots & \sum_{i=1}^{n}\frac{1}{R_{qn,i}} \end{bmatrix}, \quad (14)$$

where $G_{i,i}$ components in the main diagonal of the thermal conductance matrix are defined as the sum of the conductances connected to the i^{th} node and $G_{i,j}$ is defined as the negative thermal conductances between nodes i and j. Moreover, $R_{qi,i}$ is the coolant flow resistance of fluid flow passing the node i , and $R_{qi,j\ i}$ is the coolant flow resistance of fluid flow from the node j to the node i.

V. Experimental Evaluation

A. Experimental Setup

To effectively validate and evaluate the performance of the created LPTN and to gain details about the accuracy of the method in the prediction of temperature distribution across the Machine, an experimental verification stage was carried out. The experiments conducted for the validation of the model are described in short hereafter.

For this purpose, the machine understudy run at the nominal load and speed. The tested motor is equipped by the RTD PT100 sensors to measure the temperatures of the windings, inlet cooling air, outlet-cooling air, and the ambient.

B. Comparison of Thermal Modeling Results and Experimental Results

Table I shows the steady-state analysis of LPTN at nominal load and speed. Accordingly, the hottest point is located at the end winding in the outlet region of the machine by the temperature around 112.5 (°C).

TABLE I

Steady-state Temperature of nodal point of LPTN under Nominal Load and Speed

Node	Temperature (°C)
Stator end wind in inlet flow region (Plane D)	107.1
Coil winding Temperature in Plane B	105,7
Stator end winding in the outlet region (Plane E)	112,5
Stator yoke in inlet region (Plane A)	97,4
Coil winding in the upper part of Plane A	106,8
Middle coil temperature in Plane B	103,6
Coil winding in down near the air gap in Plane A	100,4
Stator teeth temperature in Plane A	98,8
Outlet Air temperature	41.1

During the test, the inlet cooling air temperature was 32 (°C), and the ambient temperature was 28.3 (°C). The machine rotational speed was 1500-rpm, and the volumetric cooling air flow rate was 3.7 (m^3/s). Table II shows the calculated and measured stator winding, and the outlet cooling air temperatures. It is essential to know that the stator winding temperature is the average temperature of the windings of three phases.

TABLE II

Analytical and Experimental Results

Location	Analytical Results (°C)	Experimental Results (°C)
Stator windings	103.6	104.8
Outlet cooling Air	41.1	42.9

Accordingly, it can be concluded that there is a good agreement between the analytical and experimental results.

VI. Conclusion

This paper provided the analytical thermal analysis method for the high power salient pole synchronous machine by using multi-model planes method. To achieve the objectives established, the analytical LPTN thermal model was selected as an ideal method to analyze the heat transfer of the machine. The basic principles of heat transfer were presented. In addition, common correlations, as well as critical parameters in the thermal calculation, were demonstrated and summarized and different methods to overcome these challenges were proposed.

Finally, the proposed thermal model was validated experimentally. The comparison shows close agreement between the thermal models and the measurements data,

VII. References

[1] A. Boglietti, A. Cavagnino, D. Staton, M. Shanel, M. Mueller, and C. Mejuto, "Evolution and Modern Approaches for Thermal Analysis of Electrical Machines," IEEE Trans. Ind. Electron., vol. 56, no. 3, pp. 871–882, Mar. 2009.

[2] C. Mejuto, "Improved lumped parameter thermal modelling of synchronous generators," The University of Edinburgh, 2010.

[3] C. Micallef, "End winding cooling in electric machines," 2006.

[4] P. Shams Ghahfarokhi, A. Kallaste, A. Belahcen, and T. Vaimann, "Analytical thermal model and flow network analysis suitable for open self-ventilated machines," IET Electr. Power Appl., Feb. 2020.

[5] A. Boglietti, A. Cavagnino, and D. Staton, "Determination of Critical Parameters in Electrical Machine Thermal Models," IEEE Trans. Ind. Appl., vol. 44, no. 4, pp. 1150–1159, 2008.

[6] S. Nategl, D. Lindberg, O. Aglen, R. Brammer, and A. Boglietti, "Review and Trends in Traction Motor Design: Electromagnetic and Cooling System Layouts," in Proceedings - 2018 23rd International Conference on Electrical Machines, ICEM 2018, 2018, pp. 2600–2606.

[7] A. Boglietti, S. Nategh, E. Carpaneto, L. Boscaglia, and C. Scema, "An optimization method for cooling system design of traction motors," in 2019 IEEE International Electric Machines and Drives Conference, IEMDC 2019, 2019, pp. 1210–1215.

[8] C. Scema, S. Nategh, A. Boglietti, L. Boscaglia, and D. Ericsson, "A hybrid thermal modeling method for traction motors used in duty-cycles," in 2019 IEEE International Electric Machines and Drives Conference, IEMDC 2019, 2019, pp. 2132–2137.

[9] G. Traxler-Samek, R. Zickermann, and A. Schwery, "Cooling airflow, losses, and temperatures in large air-cooled synchronous machines," IEEE Trans. Ind. Electron., vol. 57, no. 1, pp. 172–180, Jan. 2010.

[10] M. Satrústegui De Legarra, "Thermal and hydraulic design of water-based cooling systems for electrical machines," University of Navarra, 2017.

[11] J. Nerg and V. Ruuskanen, "Lumped-parameter-based thermal analysis of a doubly radial forced-air-cooled direct-driven permanent magnet wind generator," Math. Comput. Simul., vol. 90, pp. 218–229, 2013.

[12] J. Nerg, M. Rilla, and J. Pyrhönen, "Thermal analysis of radial-flux electrical machines with a high power density," IEEE Trans. Ind. Electron., vol. 55, no. 10, pp. 3543–3554, 2008.

[13] J. A. Malumbres, M. Satrustegui, I. Elosegui, J. C. Ramos, and M. Martínez-Iturralde, "Analysis of relevant aspects of thermal and hydraulic modeling of electric machines. Application in an Open Self Ventilated machine," Appl. Therm. Eng., vol. 75, pp. 277–288, Jan. 2015.

[14] P. H. Mellor, D. Roberts, and D. R. Turner, "Lumped parameter thermal model for electrical machines of TEFC design," IEE Proc. B Electr. Power Appl., vol. 138, no. 5, p. 205, 1991.

[15] C. Mejuto, M. Mueller, M. Shanel, A. Mebarki, M. Reekie, and D. Staton, "Improved synchronous machine thermal modelling," in Proceedings of the 2008 International Conference on Electrical Machines, ICEM'08, 2008.

[16] C. Mejuto, M. Mueller, M. Shanel, A. Mebarki, and D. Staton, "Thermal modelling investigation of heat paths due to iron losses in synchronous machines," in IET Conference Publications, 2008, no. 538 CP, pp. 225–229.

[17] P. Shams Ghahfarokhi, A. Kallaste, T. Vaimann, and A. Belahcen, "Thermal Analysis of Totally Enclosed Fan Cooled Synchronous Reluctance Motor-state of art - IEEE Conference Publication," in IECON 2019 - 45th Annual Conference of the IEEE Industrial Electronics Society, 2019, pp. 1–5.

[18] P. Shams Ghahfarokhi, A. Kallaste, A. Belahcen, T. Vaimann, and A. Rassõlkin, "Hybrid thermal model of a synchronous reluctance machine," Case Stud. Therm. Eng., vol. 12, pp. 381–389, Sep. 2018.

[19] M. Popescu, D. Staton, D. Dorrell, F. Marignetti, and D. Hawkins, "Study of the thermal aspects in brushless permanent magnet machines performance," in 2013 IEEE Workshop on Electrical Machines Design, Control and Diagnosis (WEMDCD), 2013, pp. 60–69.

[20] P. Shams Ghahfarokhi, "Development of Thermal Analysis Tools for Synchronous Reluctance Motors - TalTech raamatukogu digikogu," Tallinn University of Technology, 2019.

[21] P. Shams Ghahfarokhi, A. Belahcen, A. Kallaste, T. Vaimann, L. Gerokov, and A. Rassolkin, "Thermal analysis of a SynRM using a thermal network and a hybrid model," in Proceedings - 2018 23rd International Conference on Electrical Machines, ICEM 2018, 2018, pp. 2682–2688.

[22] Y. Gai et al., "Cooling of automotive traction motors: Schemes, examples, and computation methods," IEEE Trans. Ind. Electron., vol. 66, no. 3, pp. 1681–1692, Mar. 2019.

[23] P. Shams Ghahfarokhi, A. Kallaste, T. Vaimann, A. Rassolkin, and A. Belahcen, "Determination of natural convection heat transfer coefficient over the fin side of a coil system," Int. J. Heat Mass Transf., vol. 126, pp. 677–682, Nov. 2018.

[24] P. S. Ghahfarokhi, A. Kallaste, T. Vaimann, and A. Belahcen, "Natural convection from flat side's of coil system," in 2018 19th International Scientific Conference on Electric Power Engineering, EPE 2018 - Proceedings, 2018, pp. 1–5.

[25] C. Mejuto, "Improved lumped parameter thermal modelling of synchronous generators," 2010.

[26] C. K. Stimpson, J. C. Snyder, K. A. Thole, and D. Mongillo, "Roughness effects on flow and heat transfer for additively manufactured channels," J. Turbomach., vol. 138, no. 5, May 2016.

[27] C. Gazley, "Heat transfer characteristics of the rotational and axial flow between concentric cylinders," J. Heat Transf., no. 80, pp. 79–90, 1958.

[28] K. Takahashi, H. Kuwahara, K. Kajiwara, and T. Obata, "Airflow and thermal conductance in a totally enclosed induction motor," Heat Transf. - Asian Res., vol. 31, no. 1, pp. 7–20, Jan. 2002.

[29] G. E. Luke, "The Cooling of Electric Machines," Trans. Am. Inst. Electr. Eng., vol. 42, pp. 636–652, Jan. 1923.

[30] F. P. Incropera, D. P. DeWitt, T. L. Bergman, and A. S. Lavine, Fundamentals of Heat and Mass Transfer. 2007.

[31] P. Shams Ghahfarokhi, A. Kallaste, T. Vaimann, A. Rassolkin, and A. Belahcen, "Steady-state thermal model of a synchronous reluctance motor," in 2018 IEEE 59th Annual International Scientific Conference on Power and Electrical Engineering of Riga Technical University, RTUCON 2018 - Proceedings, 2018.

VIII. Biographies

Payam Shams Ghahfarokhi was born in Iran, in 1986. He received a B.Sc. degree in electrical power engineering from IAUN, Iran, in 2010, an M.Sc. degree in electrical power engineering from Newcastle University, UK, in 2011, and the Ph.D. degree in electrical engineering and machines from Tallinn University of Technology, Estonia, 2019. He is currently lead researcher and postdoc research at Riga Technical University, Latvia His main field of interests is the design of PM and Synchronous Reluctance electrical machine and thermal design of the electrical machine.

Ants Kallaste was born in Pärnu, Estonia in 1980 and received his B.Sc., M.Sc., and Ph.D. degrees in electrical engineering from Tallinn University of Technology, Estonia, in 2004, 2006, and 2013, respectively. He is currently a Senior Researcher in Tallinn University of Technology, Department of Electrical Engineering and carrying out postdoctoral research at the Department of Electrical Engineering and Automation, Aalto University, Espoo, Finland. He has been working in several companies as an Electrical Engineer. Presently he is working at the Tallinn University of Technology, Department of Electrical Engineering holding the position of Head of Chair of Electrical Machines. He has been the IEEE member since 2013. His main research interests include permanent magnet machine design and wind turbines.

Andrejs Podgornovs received the B. Sc. ing. (2001), M. Sc. ing. (2004) Rigas Technical University, Riga, Latvia, all in electrical engineering. He received Dr. sc. ing. (2009) degree in Riga Technical University, in the field of electrical engineering. He is associate professor (from 2015) of RTU. Main research interests are electric power supply quality assessments, electrical measurements, and mathematical calculations.

Anouar Belahcen (M13-SM15) received the M.Sc. (Tech.) and Doctor (Tech.) degrees from Helsinki University of Technology, Finland, in 1998, and 2004, respectively. He is now Professor of electrical machines at Tallinn University of Technology, Estonia and Professor of Energy and Power at Aalto University, Finland. His research interest are numerical modeling of electrical machines, magnetic materials, coupled magneto-mechanical problems, magnetic forces, magnetostriction, and fault diagnostics

Toomas Vaimann (S'11-M'14) was born in Pärnu, Estonia, in 1984 and received his B.Sc., M.Sc., and Ph.D. degrees in electrical engineering from Tallinn University of Technology, Estonia, in 2007, 2009. and 2014, respectively. He is currently a Senior Researcher in Tallinn University of Technology, Department of Electrical Engineering and carrying out postdoctoral research at the Department of Electrical Engineering and Automation, Aalto University, Espoo, Finland. He has been working in several companies as an Electrical Engineer. He is the member of IEEE, Estonian Society of Moritz Hermann Jacobi and Estonian Society for Electrical Power Engineering. His main research interest is the diagnostics of electrical machines.

Oleg Kudrjavtsev was born in Tallinn, Estonia, in 1986. He received B.Sc., M.Sc., and Ph.D. degrees from Tallinn University of Technology in 2008, 2010, and 2017, respectively. His research activities cover PM generators for wind turbines. He has worked in electrical industry for 5 years covering testing, maintenance and design of electrical machines as Electrical Engineer in Konesko AS. His responsibilities included design of induction motors and permanent magnet generators for small wind turbines. Currently he works in ABB AS Electrical Machines Factory, where he is a R&D project manager.

This is a post-print of a paper published in Proceedings of the 2020 International Conference on Electrical Machines (ICEM 2020) and is subject to IEEE copyright.
https://doi.org/10.1109/ICEM49940.2020.9270753
Electronic ISBN: 978-1-7281-9945-0.
Print on Demand (PoD) ISBN: 978-1-7281-9946-7.